IMPACT OF LOAD ON WINDING INDUCTANCES OF PERMANENT MAGNET GENERATORS WITH MULTIPLE DAMPING CIRCUITS USING ENERGY PERTURBATION

A.A. Arkadan, Student Member N.A. Demerdash, Senior Member
Clarkson University
Potsdam, New York

J.G. Vaidya, Senior Member M.J. Shah, Non Member
Sundstrand Corporation
Rockford, Illinois

Abstract: In this first of a set of two companion papers on the modeling of permanent magnet generators in the natural abc frame of reference, a computer-aided method to determine the impact of load on winding inductances and other machine parameters of permanent magnet generators with multiple damping circuits is presented. The method is general in nature so that it can be applied to detailed computer-aided design processes of permanent magnet generator systems. The method is based on use of the abc frame of reference for development of the necessary state equations. This is an advantage over other methods that employ Park's direct-quadrature transformation in obtaining a machine state model in the dq0 frame of reference in that no simplifying assumptions, such as neglect of magnetic nonlinearities, neglect of space harmonics in the mmfs as well as space harmonics in flux density waveforms or winding flux linkages, are necessary in this approach. The effects of magnetic saturation and inherent harmonics in flux linkages on machine parameters are accounted for by obtaining a series of comprehensive finite element magnetic field solutions throughout the machine cross-section. These solutions cover a complete ac cycle of the armature current under any load conditions. The saturated values of the self and mutual inductances for the various machine windings are calculated directly from magnetic field solutions using an energy perturbation approach. These inductances are utilized, in addition to the induced back emfs, which are in turn calculated from the field solutions, in the resulting state model of the permanent magnet generator in the natural abc frame of reference. The method is applied to a two pole, 75 KVA, 208V, 24000 r/min permanent magnet generator with multiple damping circuits.

INTRODUCTION

Permanent magnet generators, including ones with multiple damping circuits, have significant potential in many applications of power generation such as in wind power generation, small hydroelectric power generation, and solar dynamic power generation. Potential applications in the aerospace and marine areas also exist. In some of these applications very high rated speeds may be necessary for purposes of minimizing weights and volumes of such permanent magnet generators. This necessitates the use of state of the art materials, and computer-aided design tools.

Previous methods of dynamic generator analysis, including those of analyzing the transient characteristics of permanent magnet generators, centered on use of conventional dq0 type models [1-4]. These methods do not address the effects of space harmonics in mmfs and flux linkages, or the effects of time harmonics in armature currents and voltages, on the dynamics of such generators, particularly when such generators are interfaced with electronically switched loads. Consequently, new numerical methods are needed which are capable of predicting the transient and dynamic performance of such permanent magnet (PM) generator systems with greater accuracy, including the impact of their damping circuits on the machine system dynamics. Greater attention to effects of space harmonics in flux linkages and time harmonics in currents and voltages, on the performance of such generators was required by the nature of the applications. Furthermore, it should be noted that when the load of such a machine is changed, the operating point of the overall magnetic circuit changes, and consequently, changes take place in the values of the winding inductances including those of the damping circuits. This is due to changes in the demagnetization effect of the armature reaction on the whole magnetic circuit of a PM generator when load changes. It should be pointed out that such armature reaction effects become more considerable in this type of generator in which permanent magnets are used for excitation instead of an excitation field winding. This is because in this type of design, the field excitation can not be regulated, unlike that in the case of a machine with a rotor equipped with a wound field.

Accordingly, in this first in a set of two companion papers, a computer -aided method for studying the impact of load on winding inductances of PM generators with multiple damping circuits is presented. This method is applied in a simultaneous companion paper in this set [5] to study the transient performance of a 2 pole, 75 KVA, 208V, 24000 r/min, permanent magnet generator with multiple damping circuits. Figure (1) shows a cross-section of the machine. A collar (damping ring) is fitted around the

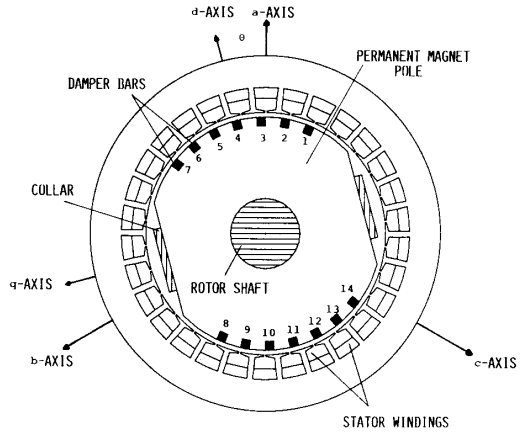

CROSS-SECTION OF A 24000 r/min, 75 KVA, 2 POLE PERMANENT MAGNET GENERATOR

Figure(1)

88 WM 001-0 A paper recommended and approved tby the IEEE Rotating Machinery Committee of the IEEE Power Engineering Society for presentation at the IEEE/PES 1988 Winter Meeting, New York, New York, January 31 - February 5, 1988. Manuscript submitted September 1, 1987; made available for printing November 13, 1987.

0885-8969/88/1200-0880$01.00©1988 IEEE

rotor, which acts as a shorted coil. The collar aids the damping effects caused by the 14 damper bars which are embedded in the two pole faces of the rotor's permanent magnets. The method is based on use of the natural abc frame of reference for the development of the necessary state equations. The parameters of this state model (winding inductances) are computed as shown in this paper using a combined energy perturbation-finite element field computation technique [10,11]. The state model derived in this paper was applied, in conjunction with the methods of IEEE Standard #115 [6], in the determination of steady state inductances, and subtransient inductances and time constants of the above mentioned permanent magnet generator, and the study of the effects of various generator faults on generator transient characteristics, as detailed in a simultaneous companion paper, reference [5]. In a future paper [7], the natural abc frame of reference method developed here will be used in the study of the characteristics of the permanent magnet generator at hand when feeding on electronically switched dc (rectified) load, as well as in studying the effects of electronic component failure in rectifier bridges on the generator-rectifier -load system.

This method accounts for the effects of magnetic nonlinearities and space harmonics, as well as saliency, effects of loading and damping circuits on the dynamic and transient performance of PM generators by obtaining a series of magnetic field solutions at various rotor positions covering the 360 electrical degree cycle for each studied load condition. These field solutions result in Fourier series type expressions of the saturated self and mutual incremental inductances for the different machine windings including those of the damper windings. These Fourier type expressions of the inductances are determined in this paper in conjunction with induced back emf Fourier type expressions in the abc frame state model to account for saliency, saturation, and damping effects in the PM generator performance. Furthermore, a verification of a sample of these computed inductances by comparison to experimental data is given. Finally, the abc armature data is used in the calculation of direct and quadrature axis inductances under different load conditions.

THE NATURE OF THE STATE MODEL OF PERMANENT MAGNET GENERATORS WITH MULTIPLE DAMPER CIRCUITS IN THE NATURAL abc FRAME OF REFERENCE

A lumped parameter state model in the natural abc frame of reference for transient analysis of permanent magnet generators, Figure (1), which is based upon an eight-winding representation, which reduces to a seven-winding representation, is derived. Three windings represent the three armature phases a, b, and c. The fourth winding, f, is a fictitious winding, which represents the rotor mounted permanent magnet excitation system by an equivalent field winding with a constant fictitious excitation current, i_f (permanent magnet coercivity, H_c, is constant, and hence equivalent magnet mmf is also constant). The effect of the fictitious field winding, with its constant field current, on the model will also be shown here, and because i_f = constant it is not one of the state variables in this model. The fifth and sixth windings, kd and kq, represent the effects of the damper bars embedded in the pole faces of the permanent magnet rotor. The seventh and eighth windings, sd and sq, represent the damping effects of the metallic collar (damping ring) surrounding the rotor, whose magnetic axis is the direct axis of the rotor.

The differential equations used to model the transient and dynamic performance of electrical machines in general, and 3 phase machines in particular, are derived from the interaction between the armature phase windings, field windings, and damping windings. Accordingly, for a j^{th} winding in a system of 8 magnetically coupled coils in a given machine, a, b, c, f, kd, kq, sd, and sq, one can write the following for the terminal voltage of the j^{th} coil, using the well known consumer (load) system of electric network notation [16]:

$$v_j = r_j i_j + \{\sum_k [(\partial\lambda_j/\partial i_k)(di_k/dt)]\} + [(\partial\lambda_j/\partial\theta)(d\theta/dt)] \quad (1)$$

Here, j, k = a, b, c, f, kd, kq, sd, and sq. Also, here r_j is the ohmic resistance of the j^{th} winding, λ_j is its flux linkage, and θ is the rotor position angle measured from a fixed frame of reference, Figure (1). However, the term $(\partial\lambda_j/\partial i_k)$ is the incremental inductance term, L_{jk}^{inc}. Also, the term $(d\theta/dt) = \omega$ is the angular speed of the rotor in rad/s.

The first term on the right hand side of equation (1) represents the ohmic voltage drop. Meanwhile, the second term represents the transformer voltage, and the last term represents the rotational voltage. This last term, the rotational (motional) voltage induced in the j^{th} winding can be attributed to the effects of rotating magnetic field components due to; (a) rotor mounted permanent magnets (fictitious field winding), (b) the currents in the armature windings, and (c) the induced currents in the damper windings.

In the case of modeling permanent magnet generators of the type under consideration, the state model of equation (1) can be used excluding the state equation corresponding to the fictitious field winding whose associated current, i_f = constant. This is because i_f is no longer a state variable. Accordingly, the rotational voltage term, $[(\partial\lambda_j/\partial\theta)(d\theta/dt)]$, can be decomposed into two components. These components are rotational voltages due to the permanent magnet flux, e_j, and the rotational voltages due to rotating flux components produced by the armature and damper windings currents which is explained next. For further details reference [8] should be consulted. Accordingly, the model of equation (1) can be written as follows:

$$v_j = r_j i_j + \sum_k [L_{jk}^{inc}(di_k/dt)] + \sum_k \omega i_k \frac{d}{d\theta}(L_{jk}^{inc})] + e_j \quad (2)$$

where j, k = a, b, c, kd, kq, sd, and sq. Here, the third term on the right hand side of equation (2) represents the rotational voltage of winding j due to the armature winding currents, and the damper winding currents. Again, the last term, e_j, represents the contribution of the permanent magnet flux to the rotational voltage induced in the j^{th} winding, which is the no-load induced back emf, for further details references [8] and [9] should be consulted.

Accordingly, dropping the superscript "inc" from the various inductance terms, one can use equation (2) to write in expanded matrix form the following state model, which governs the electrical transients associated with permanent magnet generators with multiple damping circuits [8]:

$$\begin{bmatrix} v_a \\ v_b \\ v_c \\ v_{kd} \\ v_{kq} \\ v_{sd} \\ v_{sq} \end{bmatrix} = \begin{bmatrix} r_a & 0 & 0 & 0 & 0 & 0 & 0 \\ 0 & r_b & 0 & 0 & 0 & 0 & 0 \\ 0 & 0 & r_c & 0 & 0 & 0 & 0 \\ 0 & 0 & 0 & r_{kd} & 0 & 0 & 0 \\ 0 & 0 & 0 & 0 & r_{kq} & 0 & 0 \\ 0 & 0 & 0 & 0 & 0 & r_{sd} & 0 \\ 0 & 0 & 0 & 0 & 0 & 0 & r_{sq} \end{bmatrix} \begin{bmatrix} i_a \\ i_b \\ i_c \\ i_{kd} \\ i_{kq} \\ i_{sd} \\ i_{sq} \end{bmatrix} + \omega \left\{ \frac{d}{d\theta} \begin{bmatrix} L_{aa} & L_{ab} & L_{ac} & L_{akd} & L_{akq} & L_{asd} & L_{asq} \\ L_{ba} & L_{bb} & L_{bc} & L_{bkd} & L_{bkq} & L_{bsd} & L_{bsq} \\ L_{ca} & L_{cb} & L_{cc} & L_{ckd} & L_{ckq} & L_{csd} & L_{csq} \\ L_{kda} & L_{kdb} & L_{kdc} & L_{kdkd} & L_{kdkq} & L_{kdsd} & L_{kdsq} \\ L_{kqa} & L_{kqb} & L_{kqc} & L_{kqkd} & L_{kqkq} & L_{kqsd} & L_{kqsq} \\ L_{sda} & L_{sdb} & L_{sdc} & L_{sdkd} & L_{sdkq} & L_{sdsd} & L_{sdsq} \\ L_{sqa} & L_{sqb} & L_{sqc} & L_{sqkd} & L_{sqkq} & L_{sqsd} & L_{sqsq} \end{bmatrix} \right\} \begin{bmatrix} i_a \\ i_b \\ i_c \\ i_{kd} \\ i_{kq} \\ i_{sd} \\ i_{sq} \end{bmatrix}$$

$$+ \begin{bmatrix} L_{aa} & L_{ab} & L_{ac} & L_{akd} & L_{akq} & L_{asd} & L_{asq} \\ L_{ba} & L_{bb} & L_{bc} & L_{bkd} & L_{bkq} & L_{bsd} & L_{bsq} \\ L_{ca} & L_{cb} & L_{cc} & L_{ckd} & L_{ckq} & L_{csd} & L_{csq} \\ L_{kda} & L_{kdb} & L_{kdc} & L_{kdkd} & L_{kdkq} & L_{kdsd} & L_{kdsq} \\ L_{kqa} & L_{kqb} & L_{kqc} & L_{kqkd} & L_{kqkq} & L_{kqsd} & L_{kqsq} \\ L_{sda} & L_{sdb} & L_{sdc} & L_{sdkd} & L_{sdkq} & L_{sdsd} & L_{sdsq} \\ L_{sqa} & L_{sqb} & L_{sqc} & L_{sqkd} & L_{sqkq} & L_{sqsd} & L_{sqsq} \end{bmatrix} \cdot \frac{d}{dt} \begin{bmatrix} i_a \\ i_b \\ i_c \\ i_{kd} \\ i_{kq} \\ i_{sd} \\ i_{sq} \end{bmatrix} + \begin{bmatrix} e_a \\ e_b \\ e_c \\ 0 \\ 0 \\ 0 \\ 0 \end{bmatrix} \qquad (3)$$

In order to numerically determine the currents, i_a through i_{sq}, equation (3), for any set of initial conditions, the values of the applied voltages, v_a through v_{sq}, are the forcing functions in the state model of equation (3).

BRIEF REVIEW OF THE ENERGY PERTURBATION METHOD OF INDUCTANCE COMPUTATION FROM MAGNETOSTATIC FIELD SOLUTIONS

When considering permanent magnet generators of the type at hand, one must bear in mind that the inductances are dependent on load. Hence, the necessity arises for determination of new sets of machine inductances at each load (steady state condition from which a transient starts). This class of machines are often used in supplying power to electronically switched dc loads. This directly leads to a high harmonic content in the phase currents of such generators, which causes the time rate of change of these currents (di/dt) to become higher than those encountered in conventional machines with basically sinusoidal current waveforms. Hence, in order to accurately predict the dynamic behavior of such machines, one should have accurate knowledge of the self and mutual incremental (differential) machine winding inductances, $(\partial\lambda/\partial i)$, rather than the apparent inductances (λ/i), see Figure (2). This is because one can express the induction voltage terms, $(d\lambda/dt)$, as $[(\partial\lambda/\partial i)(di/dt)]$ when saturation is an important factor, as shown earlier in equations (1) and (2).

Energy and current perturbations applied to numerical magnetic field solutions, which have been used successfully and verified experimentally in several previous investigations [10,11], form the basis of a method used for machine winding incremental inductance calculations in this work. Again, this method was first introduced in detail in the work of Nehl, Demerdash and Fouad [10,11]. Therefore, only a brief review of this approach is given here for the sake of completeness and continuity.

In order to numerically compute the incremental self inductance, L_{jj}, in equation (3) for the jth winding; j = a, b, c, kd, kq, sd, and sq, one calculates the global energy, W, at the quiescent point corresponding to a given load condition. One also computes the stored energies corresponding to the following two current perturbations, $W(i_j+\Delta i_j)$ and $W(i_j-\Delta i_j)$, where Δi_j is equal to ε% of the machine's armature current. According to the method of references [10] and [11], one substitutes the above

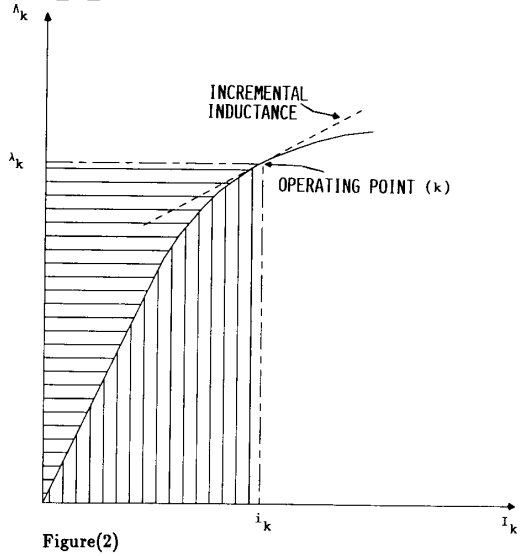

Figure(2)

FLUX LINKAGE-CURRENT CHARACTERISTIC OF k^{th} WINDING

energies in the following energy difference expression, obtained from a truncated Taylor series, for calculation of the incremental self inductance, L_{jj}:

$$L_{jj} \cong [W(i_j-\Delta i_j) - 2W + W(i_j+\Delta i_j)]/(\Delta i_j)^2 \qquad (4)$$

Next, in order to determine an incremental mutual inductance, L_{jk}, where $j \neq k$, and j, k = a, b, c, kd, kq, sd, and sq, one needs to compute four stored energies corresponding to four current perturbations. These stored energies, which are computed from magnetic field solutions are: $W(i_j+\Delta i_j,\ i_k+\Delta i_k)$, $W(i_j-\Delta i_j,\ i_k+\Delta i_k)$, $W(i_j+\Delta i_j,\ i_k-\Delta i_k)$, and $W(i_j-\Delta i_j,\ i_k-\Delta i_k)$. Again, according to the method of references [10] and [11] one substitutes the above perturbed energies in the following energy difference expression to calculate the incremental mutual inductance, L_{jk}:

$$L_{jk} \cong [W(i_j+\Delta i_j,\ i_k+\Delta i_k) - W(i_j-\Delta i_j,\ i_k+\Delta i_k) - W(i_j+\Delta i_j,$$

$$i_k-\Delta i_k) + W(i_j-\Delta i_j,\ i_k-\Delta i_k)]/(4\cdot\Delta i_j\cdot\Delta i_k) \qquad (5)$$

The expressions in equations (4) and (5) were used to determine the various self and mutual incremental inductances needed in the state model of the PM generator at hand, equation (3). The computation of these inductances are given in the following sections.

ARMATURE INDUCTANCE CALCULATION AND THE SIGNIFICANT SALIENCY EFFECTS

In this section, Fourier series type expressions for the armature windings' incremental self and mutual inductances of the PM generator, the cross-section of which is shown in Figure (1), are calculated. These expressions were used in the inductance matrix of the state model, equation (3), during the process of implementation of numerical solutions of various PM generator transients.

In order to account for loading effects on the armature's self and mutual inductances, expressions for these inductances at no load, 1 p.u. load, and 2 p.u. load were obtained. The method of obtaining these Fourier expressions of the inductances can be applied to any load condition if needed. However, in the interest of brevity only the three load cases mentioned above are given in this paper.

In order to compute the no load Fourier expressions of the incremental self and mutual inductances of the armature, finite element field solutions were obtained at sixty rotor positions covering the entire 360 electrical degree cycle. This was done by rotating the rotor at steps of 6° each, corresponding to half an armature slot pitch, thus encountering alternately the middle of a slot then the middle of a tooth successively. This is in order to have adequate representation of ripple effects due to armature slotting on the computer generated inductance data. Again, a complete field solution was performed at each of these rotor positions. Using each of these field solutions in conjunction with the energy perturbation method, the various self and mutual incremental inductances were calculated for the windings a, b, and c in the stator, at every rotor position angle in the set of sixty rotor positions. Thus, a complete profile was constructed for the variation of every armature inductance with the rotor position, from which the Fourier expressions of these inductances were extracted. Figure (3) shows a plot of the values of the incremental self inductance, L_{aa}, versus the rotor angle, θ, which was obtained at no-load. Numerical Fourier series analysis was applied to this inductance data from which a truncated Fourier type expression for $L_{aa}(\theta)$ was obtained as a function of the rotor angle, θ. Using the significant harmonic coefficients, up to the 15^{th} order, resulting from the numerical Fourier analysis of the sixty values of L_{aa} obtained from the field solutions, one obtains the following expression for $L_{aa}(\theta)$ in units of μH at no-load:

$$L_{aa}(\theta) = 29.1975 + 0.1332\sin(2\theta) - 2.1272\cos(2\theta)\ \mu H \quad (6)$$

It should be stated that this expression, as well as the remaining Fourier type inductance expressions are given here after truncating harmonic components whose magnitudes were less than 1% of the dominant component in a given expression. These truncated expressions were the ones used in the state model's numerical solutions, which will be covered in detail in a companion paper [5]. Again, the same approach was applied to compute the remaining terms of the armature's self and mutual inductances at no-load. Figure (4) shows a plot of the values of the armature's incremental mutual inductance L_{ab} obtained at no-load. Accordingly, the resulting truncated Fourier series expression for the incremental mutual inductance, $L_{ab}(\theta)$ is given as follows:

$$L_{ab}(\theta) = -14.2914 - 1.8700\sin(2\theta) + 1.0187\cos(2\theta)\ \mu H \quad (7)$$

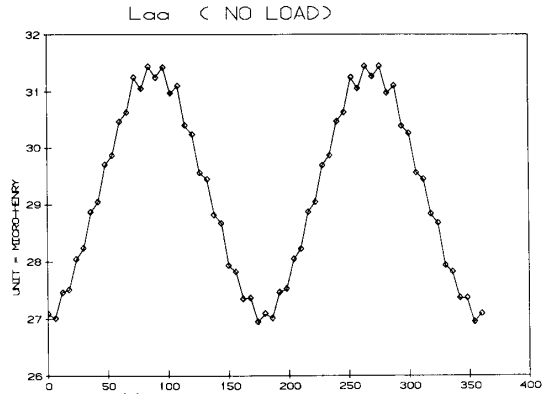

Figure(3) ARMATURE INCREMENTAL SELF INDUCTANCE VERSUS ROTOR ANGLE (NO-LOAD)

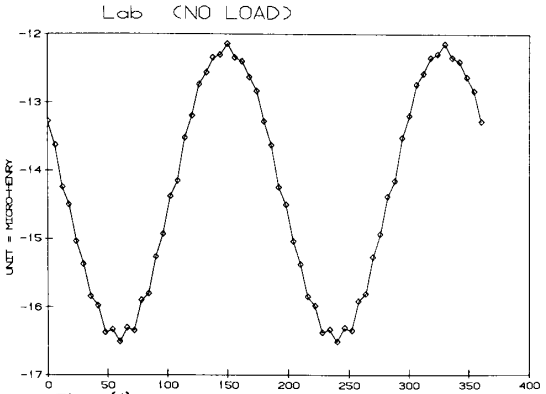

Figure(4) ARMATURE INCREMENTAL MUTUAL INDUCTANCE VERSUS ROTOR ANGLE (NO-LOAD)

The variations in the inductance profiles, Figures (3) and (4), and the expressions (6) and (7) can be attributed to one or all of the following factors:

a. The rotor position,
b. the slotting effects (slot-tooth reluctance difference), and
c. the cyclical nature of variation of the permeabilities (reluctivities) throughout the yoke.

Examination of the self inductance, $L_{aa}(\theta)$, and mutual inductance, $L_{ab}(\theta)$, data of equations (6) and (7), as well as their corresponding profiles in Figures (3) and (4), reveals an inductance variation with the angular position of the rotor of very similar nature to that which one normally encounters in conventional type machines with three phase armatures and salient pole rotors. In conventional machines with salient pole rotors, the saliency effect is due to the difference in values of magnetic circuit reluctances (permeances) along the direct (d), and quadrature (q) axes of the rotor. However, the saliency phenomenon in PM generators of the type subject of this paper is not due to differences in reluctances along the d and q axes, but is largely due to the shape of the outer boundaries of the rotor mounted permanent magnets, which helps set the profile of the radial flux density waveforms in such machines. In two pole PM generators of this type, radial flux density waveforms are consequently similar in profile to those of salient pole electromagnet machines. The resulting similarity in field distribution in PM generators of this type and those of conventional salient machines, is therefore the main reason why $L_{aa}(\theta)$ and $L_{ab}(\theta)$ exhibit the saliency effects shown and discussed above.

Meanwhile, in order to determine the effects of armature currents (load) on the incremental self and mutual inductances of the armature windings, the same process was repeated for 1.0 p.u. and 2.0 p.u. loading conditions. In this process, sixty magnetostatic field solutions were obtained at each of the loading conditions of 1.0 p.u. and 2.0 p.u. over the entire 360 electrical degree ac cycle. These magnetostatic solutions were used in conjunction with the energy perturbation method to find the armature inductances at each of the sixty rotor positions at both 1.0 p.u. and 2.0 p.u. load conditions. These armature inductance profiles for $L_{aa}(\theta)$ and $L_{ab}(\theta)$ are shown here in Figures (5) through (8) at 1.0 p.u. and 2.0 p.u. loads, in conjunction with the corresponding no-load profiles for comparison purposes. Using the same approach discussed earlier for the armature inductances under no load conditions, truncated Fourier type expressions were obtained for $L_{aa}(\theta)$ and $L_{ab}(\theta)$ and are given below for the 1.0 p.u. load case:

$$L_{aa}(\theta) = 30.454 - 0.794\sin(2\theta) - 1.564\cos(2\theta) + 0.091\sin(6\theta) - 0.035\cos(6\theta)\ \mu H \quad (8)$$

$$L_{ab}(\theta) = -14.904 - 0.889\sin(2\theta) + 1.471\cos(2\theta) - 0.046\cos(6\theta) + 0.016\cos(6\theta)\ \mu H \quad (9)$$

The truncated Fourier type expressions for $L_{aa}(\theta)$ and $L_{ab}(\theta)$ were obtained in a similar manner, and are given below for the 2.0 p.u. load case:

$$L_{aa}(\theta) = 32.206 - 0.788\sin(2\theta) - 0.322\cos(2\theta) - 0.132\sin(6\theta) - 0.157\cos(6\theta)\ \mu H \quad (10)$$

$$L_{ab}(\theta) = -15.767 + 0.107\sin(2\theta) + 0.822\cos(2\theta) + 0.066\sin(6\theta) + 0.078\sin(6\theta)\ \mu H \quad (11)$$

Notice that more significant (greater than 1% of predominant term) harmonic terms are present under load conditions than under no-load conditions of equations (6) and (7). The loading effect in changing the values of the different magnitudes of the harmonic terms in the inductance expressions from their corresponding no-load equations is clear in both the 1.0 p.u. and 2.0 p.u. cases, see Figures (5) through (8), and the expressions in equations (6) through (11).

If one consider these self and mutual armature inductances, the values of these inductances increased with the application of load (armature current). This can be physically explained, by the fact that the armature loading (armature reaction) demagnetizes the magnetic circuit (opposes permanent magnet flux), and

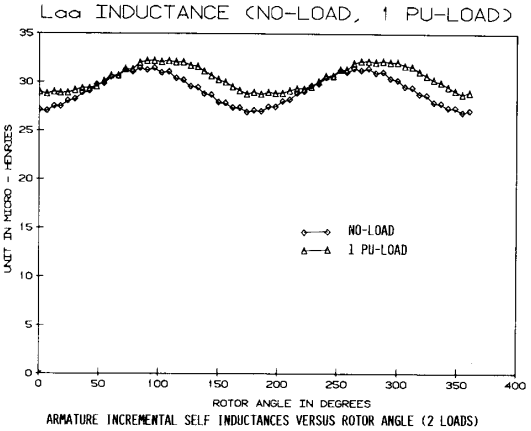

ARMATURE INCREMENTAL SELF INDUCTANCES VERSUS ROTOR ANGLE (2 LOADS)

Figure(5)

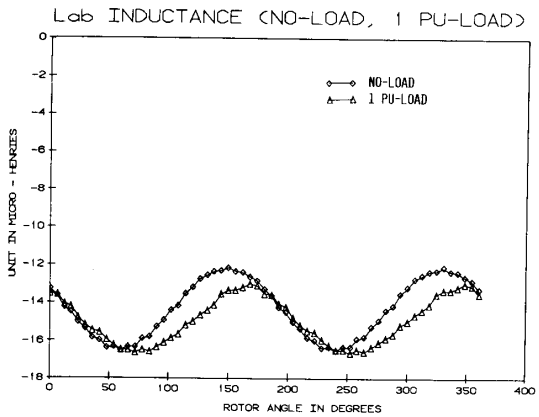

ARMATURE INCREMENTAL MUTUAL INDUCTANCES VERSUS ROTOR ANGLE (2 LOADS)

Figure(6)

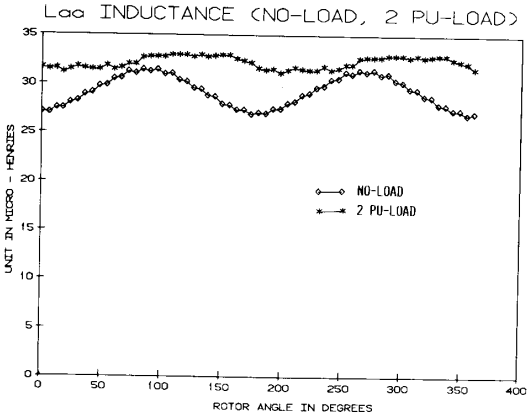

ARMATURE INCREMENTAL SELF INDUCTANCE VERSUS ROTOR ANGLE (2 LOADS)

Figure(7)

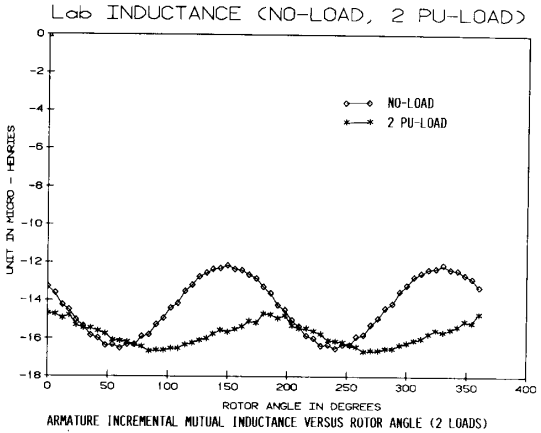

ARMATURE INCREMENTAL MUTUAL INDUCTANCE VERSUS ROTOR ANGLE (2 LOADS)

Figure(8)

hence helps lowering the flux densities in the airgap and throughout the magnetic circuit of the generator. Thus, the armature reaction (mmf) helps increase the permeabilities throughout the ferromagnetic parts of the machine, hence it lowers the reluctance of the overall magnetic circuit. Thus, it moves the quiescent point (operating point) of the machine's magnetic circuit towards the less saturated part of the λ-I characteristics of Figure (2). Accordingly, the incremental inductances which are the slopes of

such λ-I characteristics at a given operating point increase due to armature reaction, that is loading of the armature. A validation of the above findings based on experimentally obtained data on this PM generator is given next.

VERIFICATION OF COMPUTED INDUCTANCES BY COMPARISON TO EXPERIMENTAL DATA

In this section, the computed waveforms of the armature phase voltage, was obtained at no-load from finite element magnetostatic field solutions in the PM generator. This armature voltage waveform which was computed at no-load is compared here with the measured voltage waveform for the permanent magnet generator at hand, for purposes of validation of the numerical results presented in this paper. Figure (9) represents the computer simulated waveform (CSWF) of the armature phase (a) voltage under no-load at 24000 r/min as obtained from airgap magnetic vector potentials (mvps) resulting from magnetostatic field solutions. Here, the fundamental has a value of 67.84 mV/rad/s (rms), Table (1). Meanwhile, Figure (10) represents the measured (test) armature phase voltage at no-load at 16000 r/min. Here, the fundamental has a value of 67.525 mV/rad/s (rms), Table (1). This confirms the validity of the calculated values of the machine voltages, flux linkages and flux. This machine voltage was used next to verify the values of the incremental inductances obtained above. This is done by calculating the value for the fictitious inductance, L_{afm}, which is the maximum mutual inductance between an armature phase and the fictitious field winding (permanent magnet surface current). The rms value of the fundamental of the generator emf can be expressed in terms of the mutual inductance between the armature phase winding and the fictitious field winding, $L_{af}(\theta)$, according to the following conventional and well known expression [12]:

$$e_a = \omega i_f [d\{L_{af}(\theta)\}/d\theta]/\sqrt{2} \quad \text{V rms} \qquad (12)$$

where, ω is the angular frequency in rad/s, i_f, is the field current, and $L_{af}(\theta) = L_{afm} \cos(\theta)$, where $\theta = \omega t$. Since the machine at hand has a permanent magnet field, the fictitious excitation field current, i_f, was taken as the equivalent permanent magnet current sheet. Substituting the proper values for i_f, and ω into the amplitude of the voltage in equation (12) and the measured fundamental value emf per radian per second, e_a/ω = 67.525 V/rad/s, one obtains L_{afm} = 4.535 μH, Table (2). Next, the value of L_{afm} was computed using magnetostatic field solutions in conjunction with the energy perturbation method. This was done by aligning the d-axis of the rotor with the axis of phase (a), and a magnetic field solution was performed at no-load. This was followed by application of the energy perturbation method from which the peak value of $L_{af}(\theta)$, that is L_{afm} was obtained. This process yielded a value of L_{afm} = 4.464 μH, Table (2). Comparing these two numbers of L_{afm}, given in Table (2), a difference of less than 2% exists between the two results. This confirms that the computed values of the incremental inductance, L_{afm}, obtained from the energy perturbation method correlates very well with experimentally based data, and hence is a valid one. Also, this confirms that other computed values of incremental inductances for the different machine windings using the same energy perturbation method (program) are physically valid numbers, as will be further evidenced by work presented in a companion paper [5].

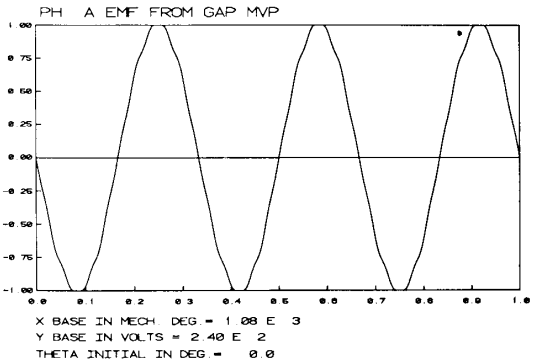

SIMULATED PHASE A EMF AT 24000 r/min AND NO-LOAD CONDITION

Figure(9)

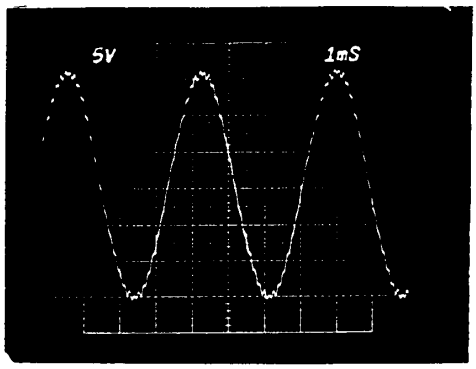

Figure(10)

MEASURED (TEST) OSCILLOGRAM OF L-N VOLTAGE AT 16000 r/min AND NO-LOAD CONDITION

No Load Voltage In mV/ rad/ s		
	Computed	Test
Fundamental	67.840 r.m.s	67.525 r.m.s

Table (1)

COMPARISON OF COMPUTED AND TEST VALUES OF FUNDAMENTAL COMPONENT OF NO-LOAD VOLTAGE

Incremental Mutual Inductance L_{afm}		
	Experimentally Based	Computer Based
L_{afm}	4.535 μH	4.464 μH

Table (2)

COMPARISON BETWEEN EXPERIMENTALLY BASED AND COMPUTED VALUES OF L_{afm}

USE OF abc ARMATURE INDUCTANCE DATA IN THE CALCULATION OF DIRECT AND QUADRATURE AXIS INDUCTANCES

Before the advent of applying computer-aided numerical methods to the analysis of electric machinery, impact of magnetic saturation on machine parameters and associated nonlinearity considerations were accounted for by empirical or semi-empirical methods [13]. Also, the equations governing the transient behavior of these machines were simplified by proper substitution (transformation) of variables, such as the use of Park's transformation and the resulting dq0 frame of reference with its associated and very well known models [13,14]. However, with advances in numerical techniques using powerful computers, one can solve directly the set of differential equations, equation (3), resulting from modeling rotating machines in the natural abc frame of

reference, without resorting to dq0 or any other transformations. This is detailed in a companion paper [5]. On the other hand, the idea of analyzing electric machines using a rotating reference (dq0) is well embedded in the literature. Accordingly, the synchronous direct and quadrature inductances, L_d and L_q, were extracted from the abc inductance expression as given below for the benefit of those readers who prefer this approach.

The values of the direct axis inductance, L_d, and the quadrature axis inductance, L_q, were calculated from the Fourier type expressions of the self and mutual inductances of the armature obtained from magnetic field solutions and energy perturbation. That is, L_d and L_q were computed using well known formulas, see references [12] and [14], as follows:

$$L_d = (L_s + M_s) + \frac{3}{2}(L_m) \tag{13}$$

$$L_q = (L_s + M_s) - \frac{3}{2}(L_m) \tag{14}$$

where, L_s and L_m are extracted from the Fourier analysis of L_{aa}, the self inductance of phase (a), which is expressable in truncated Fourier series as follows [12,14]:

$$L_{aa}(\theta) = L_s + L_m \cos(2\theta) \tag{15}$$

Here, θ is the rotor angle. Meanwhile, M_s is extracted from the Fourier analysis of the armature mutual inductance, $L_{ab}(\theta)$, which is expressable in a truncated Fourier series as follows [12,14]:

$$L_{ab}(\theta) = -[M_s + L_m \cos 2(\theta + 30°)] \tag{16}$$

The truncated expressions used for $L_{aa}(\theta)$ and $L_{ab}(\theta)$ in (15) and (16) above were obtained from the expressions given above for $L_{aa}(\theta)$ and $L_{ab}(\theta)$, equations (6) through (11). These expressions in (13) and (14) for calculation of L_d and L_q neglect flux harmonics resulting from flux components higher in order than the fundamental. This is an approximation which is inherent to the assumptions and corresponding formulation of the dq0 transformation and its associated frame of reference which is based on sinusoidal flux distributions. The values of L_d and L_q as obtained under different load conditions are given in Table (3) below. Again, the loading effect in changing the values of L_d and L_q from their corresponding no-load values is clear in both the 1.0 p.u and 2.0 p.u. cases. These direct and quadrature axes inductance values are increasing with the load as can be seen in Table (3). This phenomenon which can be attributed to the demagnetization effect of armature reaction on the overall magnetic circuit was explained above in a detailed fashion.

Using Closed Form Expressions			
	No Load	1pu	2pu
L_d	46.686 μH	47.989 μH	49.249 μH
L_q	40.291 μH	42.727 μH	46.696 μH

VALUES OF L_d AND L_q UNDER DIFFERENT LOAD CONDITIONS

Table (

COMPUTATION OF DAMPER CIRCUITS SELF AND MUTUAL INDUCTANCES

Representation of the damper bar cage in the state model of equation (3) was accomplished through an approach used earlier by Talaat [15]. In this approach, the damper bar cage was replaced by two equivalent windings, kd and kq. In a similar fashion, the metallic collar was replaced by two equivalent windings, sd and sq. Here both the kd and sd windings have their magnetic axes along the direct axis of the rotor. Meanwhile, both of the kq and sq windings have their magnetic axes along the quadrature axis of the rotor. In order to compute the self and mutual inductances associated with the four equivalent damper windings, kd, kq, sd, and sq, of the PM generator, using the above mentioned energy perturbation method, one needs to inject currents and current perturbations in the different conductors of the various current carrying windings including the damping circuits.

In order to obtain a predominent fundamental component of damper mmf along the direct axis, one distributes currents in the damper bars from a sinusoidally distributed current sheet, $C_{kd}(\theta)$ such as shown in Figure (11). This is the basis on which perturbation currents are introduced in the damper circuits. In this figure, $C_{kd}(\theta)$, is a current sheet whose peak lies along the quadrature axis, which in turn produces an mmf, $F_{kd}(\theta)$ whose peak is along the d-axis. Here, $C_{kd}(\theta)$ can be expressed as follows:

$$C_{kd}(\theta) = -C_{kdm} \cos(\frac{p}{2}\theta) \tag{17}$$

where p is the number of poles in the machine, θ is an angle measured from (-q) axis, and C_{kdm} is the peak value of the current sheet, $C_{kd}(\theta)$. Also, one can relate $C_{kd}(\theta)$ to the perturbation current, Δi_{kd}, which is the area of the current sheet between the d and q axis, as follows:

$$\int_{\frac{\pi}{2}(\frac{2}{p})}^{\pi(\frac{2}{p})} C_{kd}(\theta)\rho_k d\theta = \Delta i_{kd} \tag{18}$$

where ρ_k is the radius of an arc located in the bars at mid rotor slots, Figure (11). Substituting equation (17) into equation (18), and integrating, the amount of current injected in each of the n damper bars, Δi_{kdn}, where n = 1-14, can be related to Δi_{kd} as follows:

$$\Delta i_{kdn} = -\Delta i_{kd}[\sin(\frac{p}{2}\theta_n + \frac{\tau}{2}) - \sin(\frac{p}{2}\theta_n - \frac{\tau}{2})] \tag{19}$$

where θ_n is the angle at mid damper bar (rotor slot), n, measured from the (-q)-axis reference, and τ a distance between two adjacent damper bars, see Figure (11) for details.

In a similar manner, in order to obtain a predominent component of damper winding mmf along the quadrature axis, the currents were distributed in the damper bars from a sinusoidally distributed current sheet $C_{kq}(\theta)$, such as shown in Figure (12). Using a similar approach to the one developed for Δi_{kdn}, the

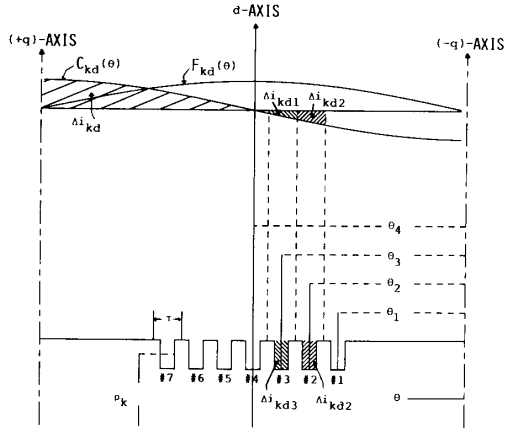

DAMPER BARS CURRENT PERTURBATION IN d-AXIS

Figure(11)

current injected in each of the damper bars, Δi_{kqn} was found as follows:

$$\Delta i_{kqn} = \Delta i_{kq}[\cos(\frac{P}{2}\theta_n + \frac{\tau}{2}) - \cos(\frac{P}{2}\theta_n - \frac{\tau}{2})] \quad (20)$$

where $\Delta i_{kq} = \Delta i_{kd}$.

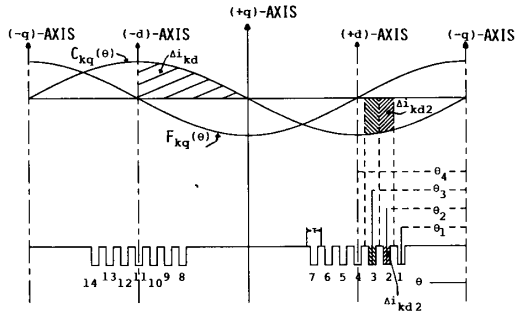

Figure(12)

DAMPER BARS CURRENT PERTURBATION DISTRIBUTION IN q-AXIS

Using the current distribution in the bars given by equations (19) and (20), the magnetic field solutions were used in conjunction with the energy perturbation method to obtain the equivalent damper bar windings' self and mutual inductances. The values of the armature to kd mutual inductance, L_{akd}, and the armature to kq mutual inductance, L_{akq}, are given at different rotor angles in Figures (13) and (14), respectively. The effect of the rotor angle on these values is clear. Full details on the remaining self and mutual inductances associated with the kd and kq windings are included in the Appendix for the no-load and 1.0 p.u. load cases. For further details reference [8] should be consulted.

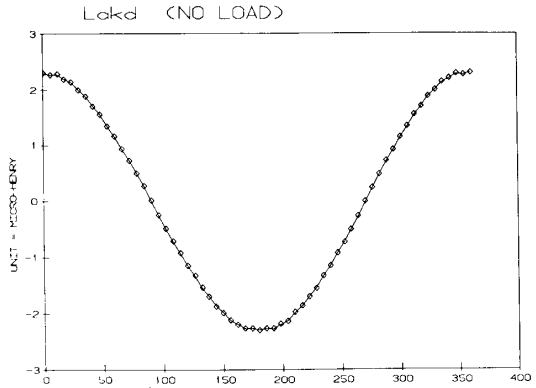

Figure(13)
INCREMENTAL MUTUAL INDUCTANCE L_{akd} VERSUS ROTOR ANGLE (NO-LOAD)

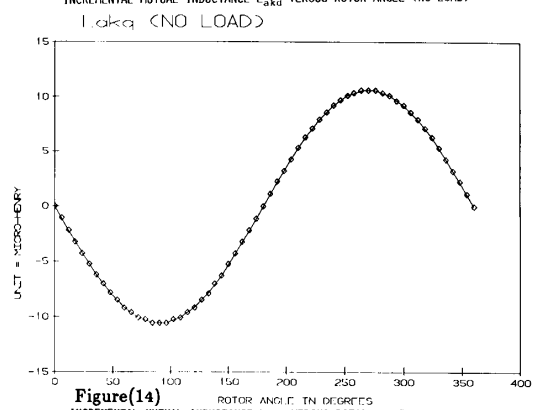

Figure(14)
INCREMENTAL MUTUAL INDUCTANCE L_{akq} VERSUS ROTOR ANGLE (NO-LOAD)

On the other hand, in order to numerically determine the incremental self and mutual inductances of the metallic collar, a collar current distribution was required. Since the collar is made of a metallic surface and has a shape as shown in Figures (15) and (16), the collar can have damping effects along both the direct and quadrature axes. In order to obtain a damping effect in the direct axis direction, the direction of flow of the induced damping current would be as shown in Figure (15). For purposes of inductance computation, the perturbation current density was accordingly injected. Thus, the perturbation current densities on the dot side and cross side are $(+\Delta i_{sd}/S_A)$ and $(-\Delta i_{sd}/S_A)$, respectively, where S_A is the cross-sectional area of the collar.

In order to obtain a damping effect along the quadrature axis direction, the induced damping current distribution would have to be as shown in Figure (17), following reasoning similar to that presented earlier in the damper bar cage case. Using steps similar to the method used in the distribution of current in the damper bars, the current sheet $C_{sq}(\alpha)$ shown in Figure (17) was integrated over a line extending from the location α_0 to α_3. Accordingly, expressions similar to those given for the perturbation currents, Δi_{kdn} and Δi_{kqn}, were derived for perturbation current distribution. For details reference [8] should be consulted. Figures (18) and (19) show the values of the incremental mutual inductances, L_{asd}, and L_{asq} at different rotor angles, respectively. Again, the effect of the rotor position (angle) is clear in these mutual inductance as expected.

The inductance values given in this section, as well as the values for the remaining inductances in equation (3), were Fourier analyzed, and accordingly Fourier type expressions were calculated, see Appendix.

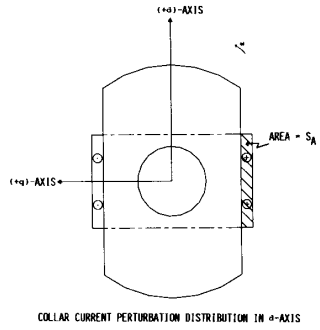

COLLAR CURRENT PERTURBATION DISTRIBUTION IN d-AXIS

Figure(15)

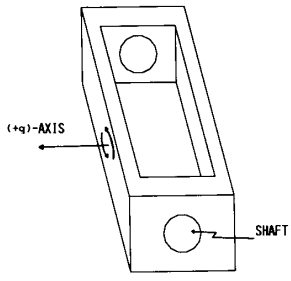

COLLAR q-AXIS DAMPING EFFECT

Figure(16)

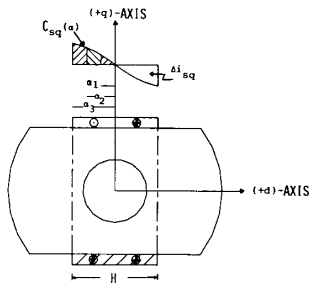

DISCRETIZATION OF HALF A COLLAR CROSS-SECTION

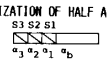

COLLAR CURRENT PERTURBATION DISTRIBUTION IN q-AXIS

Figure(17)

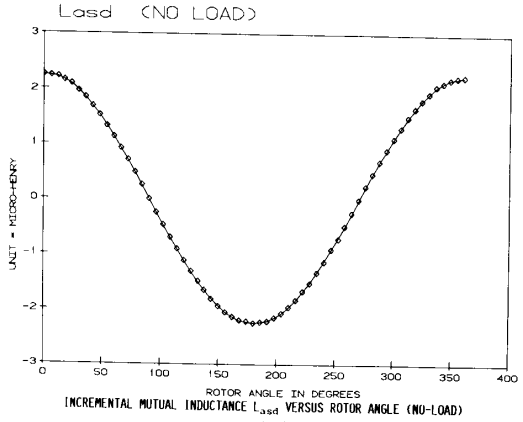

INCREMENTAL MUTUAL INDUCTANCE L_{asd} VERSUS ROTOR ANGLE (NO-LOAD)

Figure(18)

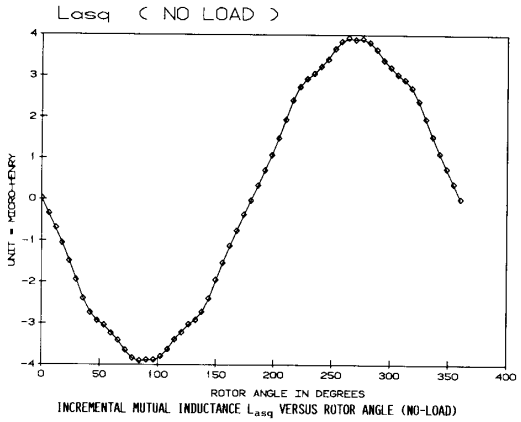

INCREMENTAL MUTUAL INDUCTANCE L_{asq} VERSUS ROTOR ANGLE (NO-LOAD)

Figure(19)

THE NATURE OF THE COMPLETE STATE MODEL OF THE PERMANENT MAGNET GENERATOR IN THE NATURAL abc FRAME OF REFERENCE AND APPLICATIONS

A method to determie Fourier type expressions for the self and mutual inductances using energy perturbations was presented and applied to a particular 75 KVA, 2-pole, 24000 r/min permanent magnet generator. Two complete sets of inductance expressions are given in the Appendix for initial conditions of no-load and 1.0 p.u. load. These inductances in conjunction with armature induced back emfs due to the permanent magnet flux, e_a, e_b, and e_c, which were computed from field solutions form the basic coefficients of the state model of the PM generator given by equation (3). Full details on the computation of these emfs from field solutions are given in reference [8]. The resulting Fourier expression of the emfs due to the permanent magnet flux for the PM generator at hand were found to be as follows:

$$e_a(\theta) = -241.17\sin(\theta) + 2.45\sin(7\theta) - 4.0\sin(11\theta) + 2.03\sin(13\theta) \quad (21)$$

$$e_b(\theta) = -241.17\sin(\theta-2\pi/3) + 2.45\sin(7\theta-2\pi/3) - 4.0\sin(11\theta-4\pi/3) + 2.03\sin(13\theta-2\pi/3) \quad (22)$$

$$e_c(\theta) = 241.17\sin(\theta-4\pi/3) + 2.45\sin(7\theta-4\pi/3) - 4.0\sin(11\theta-2\pi/3 + 2.03\sin(13\theta-4\pi/3) \quad (23)$$

Accordingly, by substituting these emf Fourier expressions into equation (3) in conjunction with a set of inductance expression corresponding to a particular load and initial conditions, one obtains a complete state model of the permanent magnet generator in the natural abc frame of reference.

This state model was used in a simultaneous companion paper [5] to study the transient performance of the generator at hand under various fault conditions. In addition, the state model was used in conjunction with the methods of IEEE Standard 115 [6] to obtain the machine's steady state inductances, and subtransient inductances and associated time constants. In the absence of an electromagnet type of field excitation no transient inductances can be defined. Furthermore, the state model will be used in a future paper [7], in the study of the characteristics of this permanent magnet generator when feeding electronically switched dc (rectified) loads, as well as in studying the effects of electronic component failure in the associated rectifier bridges on the generator-rectifier-load system.

CONCLUSIONS

A computer-aided method to determine the impact of load on winding inductances and other machine parameters of permanent magnet generators with multiple damping circuits was presented. The method was applied to a particular 2 pole, 75 KVA, 208V, 24000 r/min permanent magnet generator with multiple damping circuits. This resulted in the development of a state model in the natural abc frame of reference for computer-aided simulation for the transient characteristics of permanent magnet generators with damper windings. Fourier type expressions of the incremental self and mutual inductances, for the armature as well as the damping circuits were obtained for use in this state model. These inductance expressions which are the main coefficients in the abc state model were determined from various magnetostatic field solutions, obtained over a complete ac cycle, in conjunction with the energy perturbation method. Thus magnetic nonlinearities, space harmonics in the mmfs as well as space harmonics in flux density waveforms and winding flux linkages as well as inductances, were fully accounted for. The approach of obtaining these inductance expressions was repeated under various load conditions in order to account for generator armature loading effects. A verification of the inductance and emf values based on measured data was presented. The numerically computed data was found to be in very good agreement with the experimentally based data. Finally, this model development was used in a simultaneous companion paper to study various effects of faults, as well as to determine conventional direct and quadrature axis steady state inductances, subtransient inductances and time constants for such permanent magnet generators with rotor mounted damping circuits.

ACKNOWLEDGMENT

The authors wish to acknowledge that this work was partially funded by Sundstrand Corporation, Rockford, Illinois, under Contract No. PO B-2L34 93-247 with Clarkson University.

REFERENCES

[1] Amaratunga, G. A., Acarnley, P. P. and McLaren, P. G., "Optimum Magnetic Circuit Configurations for Permanent Magnet Aerospace Generators," IEEE Transactions on Aerospace and Electronic Systems, Vol. AES-21, No. 2, March 1985, pp. 230-255.

[2] Rahman, M. A., Osheiba, A. M., Little, T. A. and Slemon, G. R., "Effects of Samarium Cobalt Permanent Magnet on the Performance of Polyphase Hysteresis-Reluctance Motors," IEEE Transactions on Magnetics, Vol. MAG-20, No. 5, Sept. 1984, pp. 1765-1767.

[3] Richter, E. and Neumann, T. W., "Line Start Permanent Magnet Motors with Different Materials," IEEE Transactions on Magnetics, Vol. MAG-20, No. 5, Sept. 1984, pp. 1762-1764.

[4] Rahman, M. A. and Little, T. A., "Dynamic Performance Analysis of Permanent Magnet Synchronous Motors," IEEE Transactions on Power Apparatus and Systems, Vol. PAS-103, pp. 1277-1282, 1984.

[5] Arkadan, A. A. and Demerdash, N. A., "Modeling of Transients in Permanent Magnet Generators with Multiple Damping Circuits Using the Natural abc Frame of Reference," A Companion Paper, Submitted for Review and Presentation at the IEEE-PES 1988 Winter Meeting, New York.

[6] IEEE Guide: "Test Procedures for Synchronous Machines, IEEE Std. 115-1983, IEEE, Inc., 345 East 47th Street, New York, NY 10017, USA.

[7] Arkadan, A. A., Hijazi, T. M. and Demerdash, N. A., "Modeling of the Performance of a System of Electronically Rectified Load-Permanent Magnet Generator with Multiple Damping Circuits Using the Natural abc Frame of Reference," Paper Under Preparation, to be submitted for Review and Presentation at the IEEE-PES 1988 Summer Meeting.

[8] Arkadan, A. A., "Computer-Aided Dynamic Performance Prediction of Permanent Magnet Generator Systems with Damping Circuits and Electronically Switched Loads," Ph.D. Dissertation, Clarkson University, Expected December 1987.

[9] Nehl, T. W., Fouad, F. A., Demerdash, N. A. and Maslowski, E., "Dynamic Simulation of Radially Oriented Permanent Magnet Type Electronically Operated Synchronous Machines with Parameters Obtained from Finite Element Field Solutions," IEEE Transactions on Industry Applications, Vol. 1A-18, No. 2, pp. 172-182, 1982.

[10] Nehl, T. W., Fouad, F. A. and Demerdash, N. A., "Determination of Saturated Values of Rotating Machinery Incremental and Apparent Inductances by an Energy Perturbation Method," IEEE Transaction on Power Apparatus and Systems, PAS-101, 1982, pp. 4441-4451.

[11] Demerdash, N. A., Fouad, F. A. and Nehl, T. W., "Determination of Winding Inductances in Ferrite Type Permanent Magnet Electric Machinery by Finite Elements," IEEE Transactions on Magnetics, Vol. MAG-18, 1982, pp. 1052-1054.

[12] Fitzgerald, A. E., Kingsly, C. and Kusko, A., Electric Machinery, McGraw-Hill Book Company, 1971.

[13] Say, M. G., The Performace and Design of Alternating Current Machines, Pittman Press, Third Edition, 1963.

[14] Kimbark, E. W., Power System Stability: Synchronous Machines, New York, Dover Publications, Inc., 1968.

[15] Talaat, M. E., "A New Approach to the Calculation of Synchronous Machines Reactances - Part I," AIAA Transactions, April 1955, pp. 176-183.

[16] Chua, L. O. and Lin, P., Computer-Aided Analysis of Electric Circuits: Algorithms and Computational Techniques, New Jersey: Prentice-Hall, Inc., 1975.

APPENDIX

Equations (A.1) through (A.16) of this Appendix, give the Fourier type expressions of the incremental inductances of the 75 KVA PM generator at no-load in units of μH.

$$L_{aa}(\theta)=29.1975 + .1332\sin(2\theta) - 2.1272\cos(2\theta) \quad (A.1)$$

$$L_{ab}(\theta)=-14.2914 - 1.8700\sin(2\theta) + 1.0187\cos(2\theta) \quad (A.2)$$

$$L_{kdkd}(\theta) = 0.5701 \quad (A.3)$$

$$L_{akd}(\theta) = 2.3018\cos(\theta) \quad (A.4)$$

$$L_{kqkq}(\theta) = 5.2373 \quad (A.5)$$

$$L_{akq}(\theta) = -10.5942\sin(\theta) \quad (A.6)$$

$$L_{sdsd}(\theta) = 0.3735 \quad (A.7)$$

$$L_{asd}(\theta) = 2.2505\cos(\theta) \quad (A.8)$$

$$L_{sqsq}(\theta) = 4.9350 \quad (A.9)$$

$$L_{asq}(\theta) = -3.8514\sin(\theta) + .0186\cos(3\theta) \quad (A.10)$$

$$L_{kdkq}(\theta) = 0.2082E - 03 \quad (A.11)$$

$$L_{kdsd}(\theta) = 0.1982 \quad (A.12)$$

$$L_{kdsq}(\theta) = 0.6250E - 04 \quad (A.13)$$

$$L_{kqsd}(\theta) = 0.8643E - 05 \quad (A.14)$$

$$L_{kqsq}(\theta) = 1.3894 \quad (A.15)$$

$$L_{sdsq}(\theta) = 0.1370E - 03 \quad (A.16)$$

The Fourier type expressions for the remaining inductances given in equation (3) of the paper, can be directly obtained from the above expressions as detailed in reference [8].

* For biographies of authors see the companion paper, Reference [5].